

Journal of Materials Chemistry A

Accepted Manuscript



This is an *Accepted Manuscript*, which has been through the Royal Society of Chemistry peer review process and has been accepted for publication.

Accepted Manuscripts are published online shortly after acceptance, before technical editing, formatting and proof reading. Using this free service, authors can make their results available to the community, in citable form, before we publish the edited article. We will replace this *Accepted Manuscript* with the edited and formatted *Advance Article* as soon as it is available.

You can find more information about *Accepted Manuscripts* in the [Information for Authors](#).

Please note that technical editing may introduce minor changes to the text and/or graphics, which may alter content. The journal's standard [Terms & Conditions](#) and the [Ethical guidelines](#) still apply. In no event shall the Royal Society of Chemistry be held responsible for any errors or omissions in this *Accepted Manuscript* or any consequences arising from the use of any information it contains.

Cite this: DOI: 10.1039/c0xx00000x

www.rsc.org/xxxxxx

Paper

Hydrophilic separator for high performance lithium sulfur batteries

G. C. Li[†], H. K. Jing[‡], Z. Su[§], C. Lai^{*§}, L. Chen[†], C. C. Yuan[†], H. H. Li[†], L. Liu[†]

Received (in XXX, XXX) Xth XXXXXXXXX 20XX, Accepted Xth XXXXXXXXX 20XX

DOI: 10.1039/b000000x

5 Rechargeable lithium sulfur battery has been regarded as one of the most promising power source systems for the next generation EVs or HEVs. However, the low utilization of active materials, rapid capacity degradation, and poor rate capability seriously restrict its large-scale applications in commercial markets. Herein, a novel strategy, using hydrophilic separator, is reported to improve the electrochemical performance of Li-S batteries. Herein, a novel strategy, using hydrophilic separator
10 which is prepared by auto-oxidization and self-polymerization of dopamine monomer onto the surface of conventional hydrophobic separators, is reported to improve the electrochemical performance of Li-S batteries. The cells with the hydrophilic separator show significantly enhanced cycle performance. At the rate of 0.2 C, the battery demonstrates an initial capacity of 1271 mAh g⁻¹, and the capacity can still retained at 1020.3 mAh g⁻¹ after 30 cycles, which improves 77% compared with
15 the cells using conventional separators.

Introduction

The lithium sulfur battery systems, based on light-weight elements and multi-electrons redox reactions, have attracted great attention in recent years due to their high theoretical energy
20 density of 2600 Wh kg⁻¹,¹⁻⁴ which are almost one order of magnitude higher than those of conventional lithium ion batteries (LIBs). Although lithium sulfur batteries have been investigated for more than three decades,³ several major issues such as the low utilization of active material, rapid capacity degradation, and poor
25 rate capability still hinder their practical applications. Such problems that restrict the development of lithium sulfur batteries mainly result from the insulating nature of active sulfur (5×10^{-30} S cm⁻¹ at 25 °C) and the high solubility of intermediate products (Li₂S_x: 4 ≤ x < 8) in organic electrolytes which are generated
30 during the electrochemical charge/discharge processes.^{3,5,6} Recently, considerable technological strategies have been proposed to improve the reversible capacity and cycling stability for developing practical lithium sulfur batteries, including the construction of sulfur-based composites,⁷⁻²⁰ the modification and
35 protection of lithium anodes,²¹⁻²⁴ and the optimization of organic electrolytes and binders.²⁵⁻³³ Among the available attempts, the construction of sulfur-based composites, especially sulfur/carbon composites,⁷⁻¹⁵ is the most prevailing methodology, due to the good electrical conductivity and strong porous adsorption
40 capability of the conductive carbon matrix. It is observed that recent studies tend to focus on sulfur cathodes with high energy density and long cycle life, and the methods mentioned above play very important role on the improvement of electrochemical performance in lithium sulfur batteries. However, the separator,
45 as an essential component as well, which is placed between the cathode and anode to prevent the physical contact of the two electrodes as well as of which provides free lithium ionic

pathway through the micro-nanopores, was almost neglected. In fact, each component of lithium sulfur battery systems needs to
50 be studied in parallel in order to achieve optimal electrochemical performance.³⁴ In particular, the separator has an identical effect on the performance of batteries, i.e. power capability.

Work to date, the monolayer and triple-layers of micro-nanoporous polyolefin-based separators are the most widely used
55 separators for LIBs. However, polyolefin-based separators have a hydrophobic surface, which seriously hinder the adequate uptake and diffusion of organic electrolytes within the separators. Moreover, it is difficult to completely ensure the electrical isolation between the cathode and anode due to their poor thermal
60 shrinkage, leading to low capacity, poor power capability and security risks upon cycling. To address these problems, a facile dipping method to modify the polyethylene separators with mussel-inspired polydopamine (PDA) was developed by Choi and co-workers to overcome the poor compatibility of the
65 hydrophobic separators with organic electrolytes.^{35,36} After PDA treatment, a remarkably improved performance of LIBs can be obtained, as polydopamine modified separators can obtain hydrophilic properties of surfaces with constant pore structures, resulting in enhanced electrolyte uptake and electrochemical
70 performance of cells as compared to the cells using conventional hydrophobic separators.^{34,37} Herein, for the first time, we investigate the effect of polydopamine modification of separators on the electrochemical performance for lithium sulfur batteries. A simple modification method to obtain hydrophilic surface of
75 separators was conducted by dipping the separators (Celgard-2300) into alkaline solution with dissolved dopamine monomer.

Experimental

Prparation of sulfur cathodes

For the preparation of S/C composite with 60 wt% sulfur loading, carbon black (Ketjenblack EC600JD, Shanghai Fuhua Industrial Co. Ltd.) and sublimed sulfur were weighed at the mass rate of 4:6 and adequately mixed by ball-milling the mixed materials in a planetary type ball mill with a rotational speed of 300 rpm for 2 h. The mixture was then transferred into a porcelain crucible and put it into a polytetrafluorethylene (PTFE) container filled with argon. The container was heated at 155 °C for 12 h and then cooled down to room temperature, and the S/C composite was obtained. To prepare the sulfur cathodes, the S/C composite was mixed with acetylene black and PTFE at the mass ratio of 7:2:1 with ethanol as a dispersant. The mixed paste was compressed into a thin piece with a roller, cut into a disk film of 8 mm in diameter and 1.5–1.8 mg in weight, and dried in the oven at 55 °C for 12 h.

Preparation of PDA modified separators

The surface modification of separators (Celgard-2300, PP/PE/PP triple-layers) could be easily achieved by dipping the separators into the pre-prepared dopamine solution (2 mg mL⁻¹) for which Tris-HCl buffer solution (pH 8.5, 10 mM) was used as solvent. Before dipping, the separators were soaked into 50 ml methanol solution for 30 minutes, and then took out and put into the dopamine solution. The separators were then taken out after dipping for 24 h, rinsed with distilled water for several times, and dried at 30 °C for 12 h.

Materials characterization

The sulfur content in the composite was determined using a thermogravimetric analyzer (Mettler Toledo, TGA/DSC1) under Ar atmosphere with a flow rate of 50 mL min⁻¹ at a heating rate of 10 °C min⁻¹ from 30 to 600 °C. The morphology of the samples were tested using field emission scanning electron microscope (SU8010, Hitachi). FTIR spectra were recorded using an FTIR spectrometer (BIO-RAD FTS6000) in the range of ≈ 500–4000 cm⁻¹. X-ray photoelectron spectroscopy (XPS) measurements were carried out on an axis ultra (Kratos Analytical Ltd.) imaging photoelectron spectrometer using a monochromatized Al K α anode, and the C 1s peak at 284.8 eV was taken as an internal standard.

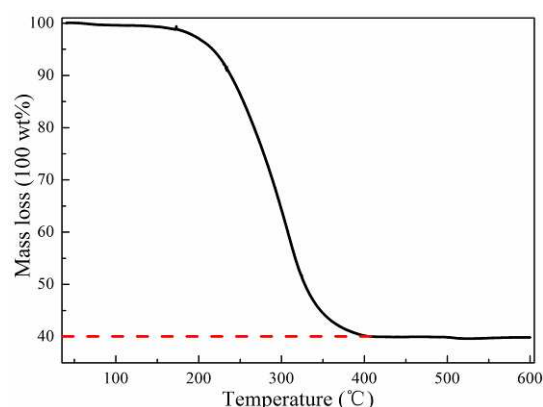
Cell assembly and electrochemical testing

The electrochemical measurements were carried out with LIR2032-coin type cells. The bare separators and the as-prepared PDA modified separators were used for the assembling of half-cells in an Ar-filled glove box for comparison, where oxygen and water content were less than 1 ppm. Lithium metal was used as the counter electrode and reference electrode. The electrolyte were mixed electrolyte salts that were comprised of 1 wt% anhydrous lithium nitrate and 1.0 M LiN(CF₃SO₂)₂ (LiTFSI) in a mixed solvents of 1,3-dioxolane (DOL) and tetra-ethylene glycol dimethyl ether (TEGDME) at the volume ratio of 1:1, which was prepared in the Ar-filled glove box as well. Galvanostatic charge/discharge tests were performed to evaluate the electrochemical capacity and cycle stability of the cells on the basis of the active sulfur at various current rate at ambient temperature under the LAND-CT2001A instrument (Wuhan Jinnuo, China). The cut-off potentials for the discharge and

charge processes were set between 1.5 and 3.0 V (vs Li/Li⁺). Cyclic voltammetry (CV) measurements were conducted using Zahner Zennium electrochemical workstation (Zahner elektrik GmbH & Co. KG) at a scan rate of 0.1 mV s⁻¹. Furthermore, electrochemical impedance spectroscopy (EIS) of the assembled half cells was measured in the discharge and charge state in the frequency range of ≈ 100 kHz–10 mHz, while the disturbance amplitude was 5 mV.

Results and discussion

The sulfur content of the as-prepared S/C composite is confirmed by thermogravimetric analysis (TGA). It can be observed from Fig. 1 that the weight loss of the composite begin from about 150 °C, and finished over 400 °C, due to evaporation of sulfur from the meso/micropores of the host carbon. The sulfur content is about 60 wt%, indicating almost no sulfur loss during the ball-milling and heat treatment process.



Scheme.1 TGA curve of the as-prepared S/C composite recorded under Ar atmosphere with a heating rate of 10 K min⁻¹.

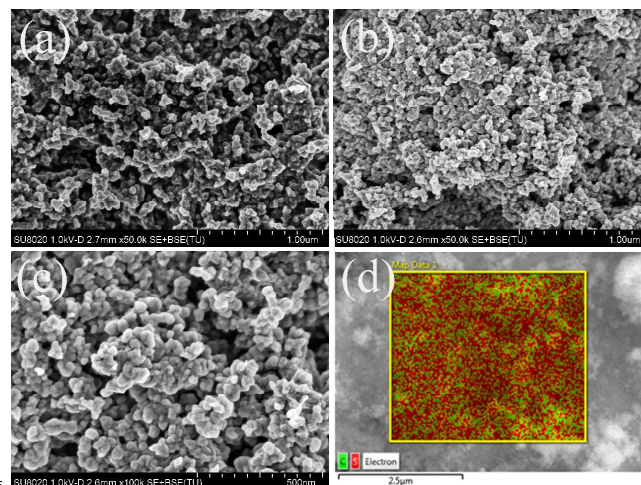


Fig. 2 SEM images of the carbon black (a) and the as-prepared S/C composites with 60 wt% sulfur (b, c); EDS element mapping of the S/C composites (d).

Scanning electron microscope (SEM) of the carbon black and S/C composite with 60 wt% sulfur are presented in Fig. 2a-c. It is shown that the carbon black appears as a loose particle aggregated of some uniform and small carbon spheres. For the S/C composite with 60 wt% sulfur loading, the aggregates

become denser and the particle size become bigger as compared to the carbon black. It is proposed that the melted sulfur with a low viscosity could be diffused and absorbed into the micro/mesopores of the carbon black by a capillary force during the heating process at 155 °C. However, when the inside pores of the carbon matrix are fully filled with sulfur, and the extra sulfur can be recrystallized on the surface of the carbon matrix, leading to denser agglomeration and bigger particle size of the S/C composite. To reveal the distribution of the sulfur and carbon, EDS element mapping are given in Fig. 2d. As presented, the sulfur and carbon are homogeneously distributed in each other, similar to previous reports.

The PDA modified separators can be successfully prepared by two simple immersion steps of taking the bare separator into the methanol solution and Tris-HCl buffer based dopamine solution orderly, as shown in Fig. 3. Polydopamine, with a molecular structure that incorporates many functional groups such as catechol, amine and imine, can be easily deposited on all types of inorganic and organic substrates, even super-hydrophobic surfaces.^{38,39} Fig. 4a presents the photographic images of the bare separator (left) and PDA modified separator (right), respectively. The formation of polydopamine experiences very complex auto-redox process as well as the generation of a series of complex intra- and inter-molecular reactions during the self-polymerization process.^{40,41} After 24 h dipping, the color of the bare separator gradually changes from white to dark brown. Fig. 4b presents a simple wetting test to verify the hydrophilic character of the PDA modified separators. As seen, after dropping an organic electrolyte [1 wt% LiNO₃ and 1.0 M LiN(CF₃SO₂)₂ dissolved in DOL/TEGDME, v/v= 1:1] onto the surface of the separator, the droplet can hardly wet the bare separator (left), whereas the PDA modified separator (right) is fully wetted immediately. It can be predicted that the cell performance by using the separator with uptake amount of liquid electrolytes would markedly improved, leading to an enhanced ionic conductivity of the PDA modified separator.^{34,37}

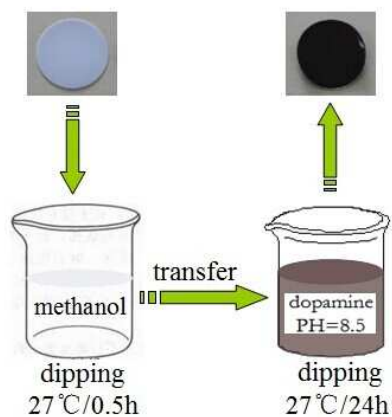


Fig. 3 The preparation process of PDA modified separators.

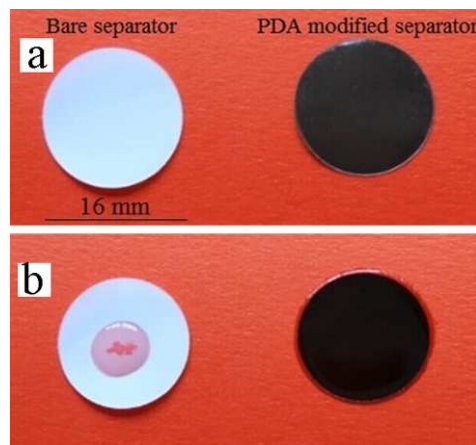


Fig. 4 (a) The photographic images of the bare separator (left) and PDA modified separator (right); (b) a simple wetting test to verify the hydrophilic character of the PDA modified separators.

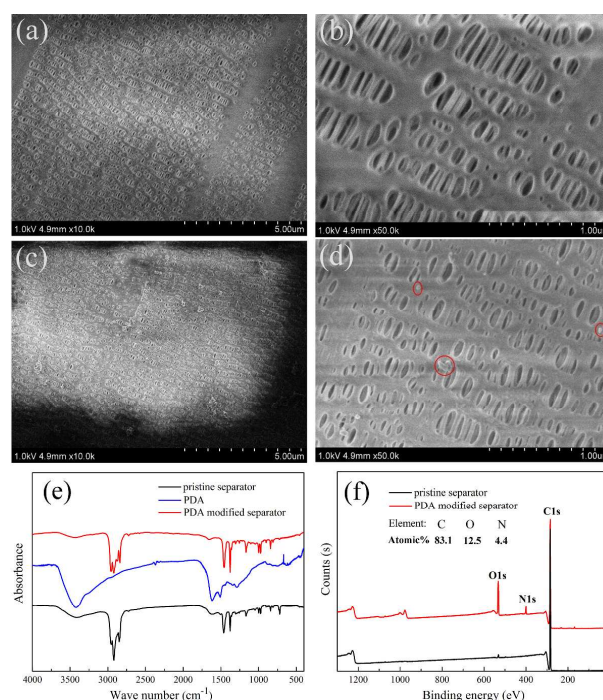


Fig. 5 The SEM images of the bare separator (a,b) and PDA modified separator (c,d) in low/high resolution. FTIR (e) and XPS spectra (f) of the PDA modified separator.

Fig. 5 presents the SEM images of the bare separator (a,b) and PDA modified separator (c,d) in low/high resolution to understand the effort of polydopamine modification on the pore structures and surface morphology of the separators. As seen in Fig. 5a and 5c in lower resolution, both of the bare separator and PDA modified separators have similar pore structures, with almost no changes in the diameters of micro/nano pores, due to the thickness of polydopamine can be accurately controlled by altering the concentration of dopamine monomer and polymerization time. Even it has already been reported that the limited thickness of the polydopamine film is no more than 50 nm.⁴² However, although very few aggregates of polydopamine nanoparticles (marked by red circle) near the pores of the PDA modified separator can be observed in high resolution SEM images of Fig. 5d, the surface morphology have no remarkable

differences between the PDA modified separator and the bare separator. In order to confirm the generation of PDA, the characterization of FTIR and XPS are conducted. As shown in Fig. 5e, for the PDA synthesized via same process without adding separator, three obvious peaks of 3426 cm^{-1} (N-H/O-H stretching vibration), 1615 cm^{-1} (C=C vibration) and 1510 cm^{-1} (N-H bending vibration) can be observed, confirming the generation of PDA.³⁷ However, for the bare separator and PDA modified separator, the characteristic peaks of PDA hardly be distinguished due to the peaks overlapping. The XPS spectra in Fig. 5f can be further confirmed the generation of PDA on the surface of celgard-2300 separator. It can be seen that only the peak of C1s can be observed, while for the PDA modified separator, two additional peaks attributed to N1s and O1s appear at 400.4 and 532.7 eV, respectively, indicating that PDA coating layer is generated on the surface of separator to produce a hydrophilic separator.

The effect of polydopamine surface modification of separators on electrochemical performance are investigated based on LIR2032 coin-type half-cells. The specific process of materials preparation and cell-assembling are completely detailed in the experimental section. Initial cyclic voltammograms (CVs) curves at a scan rate of 0.1 mV S^{-1} using PDA modified separators and bare separators for comparison, are given in Fig. 6. For the cell using PDA modified separator, two detached cathodic peak potentials at about 2.30 and 1.82 V (vs Li/Li^+) in the initial scan can be observed (Fig. 6a), which is attributed to the conversion of sulfur to high-order lithium polysulfide (Li_2S_x , $4 \leq x < 8$) and low-order lithium polysulfide to $\text{Li}_2\text{S}_2/\text{Li}_2\text{S}$.^{8,13,14,17} Meanwhile, one broad anodic peak potential at about 2.60 V can be observed, corresponding to the conversion of $\text{Li}_2\text{S}_2/\text{Li}_2\text{S}$ to lithium polysulfide and sulfur. However, for the cell using bare separator, two cathodic peak appear at about 2.25 and 1.80 V (vs Li/Li^+) (Fig. 6b), which are slightly lower than the aforementioned results. In addition, two overlapped anodic peak potentials in the voltage range of 2.6-2.7 V can be observed, suggesting a two-plateau oxidation process occurred in the anodic scan, which is different with the only one broad anodic peak potential at 2.60 V for the cell using PDA modified separator. Such a difference suggested that the hydrophilic separator has a big effect on the performance of the cells, and the enhancement of discharge-charge performance can be further illustrated below.

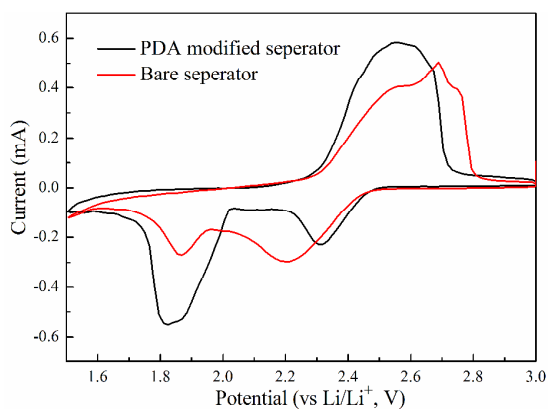


Fig. 6 Cyclic voltammograms of the cells using PDA modified separator and bare separator at a scan rate of 0.1 mV s^{-1} .

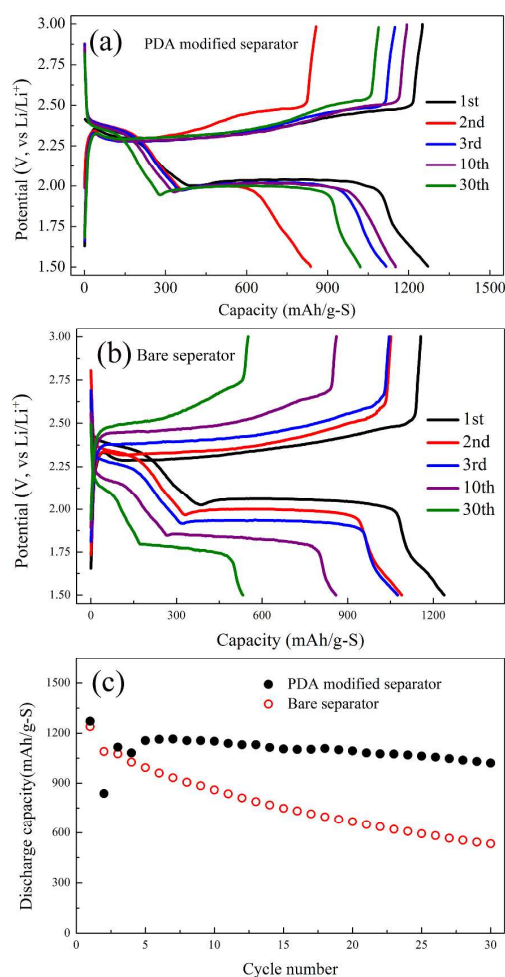


Fig. 7 The first three, 10th and 30th charge/discharge curves of the cells using PDA modified separators (a) and bare separators (b), and cycle performance (c) at the current rate of 0.2 C.

The first three, 10th and 30th charge/discharge curves of the cells using PDA modified separators and bare separators are shown in Fig. 7a and 7b, calculated at a current rate of 0.2 C based on active material sulfur. Two typical discharge potential plateau at about 2.30 V and 2.0 V (vs Li/Li^+) can be easily observed in the initial cycle for the two comparative cells, assigned to the reduction from sulfur to lithium polysulfides and further reduction to $\text{Li}_2\text{S}_2/\text{Li}_2\text{S}$ and in consistent with the CVs.¹³ For the cell using PDA modified separator, obvious decreasing of discharge capacity can be observed in the second cycle, which may relate to the dissolution of polysulfide and will be further discussed in the below. And after the second cycle, the cell will recover and its discharge performance become very stable. Correspondingly, the initial discharge capacity of the cell using PDA modified separator is 1271 mAh g^{-1} , and the final discharge capacity of 1020.3 mAh g^{-1} can be maintained at 30th cycle, as shown in Fig. 7c. In contrast, although the compared cell can deliver a high initial discharge capacity of 1238.4 mAh g^{-1} , a quick capacity-decay tendency in the subsequent cycles has also been observed. After 30 cycle, the low discharge capacity of 532.9 mAh g^{-1} is retained for the cell using bare separator, due to the solubility of lithium polysulfides and gradual aggregation of insulated Li_2S on the cathode surface during the electrochemical

reduction process. Obviously, the application of PDA modified separator in lithium sulfur batteries is more effective to improve the active sulfur utilization by extending the low discharge plateau, which is in analogy to the result reported in literature.¹³

The high-rate charge/discharge capability and cycling stability is essential for the practical application of lithium sulfur batteries. As anticipated, the cell using PDA modified separators, presented in Fig. 8a, are demonstrated a significant improvement at the current rate of 0.5 C and 1 C as compared to the cell using bare separators. The initial discharge capacities of the cells using PDA modified separators are 902.7 and 621.8 mAh g⁻¹ at 0.5 C and 1 C, respectively, whereas the initial discharge capacities of the cells using bare separators are 574.4 and 455.4 mAh g⁻¹ at 0.5 C and 1 C. In particular, the discharge capacity of 656.1 mAh g⁻¹ can still be maintained at 0.5 C after 80 cycle and 548.3 mAh g⁻¹ at 1 C after 160 cycle for the cells using PDA modified separators, which are much higher than the discharge capacity of 415.9 mAh g⁻¹ at 0.5 C and 373.5 mAh g⁻¹ at 1 C for the bare separator cells. It should be mentioned that the cell using PDA modified separator show a higher coulombic efficiency than that bare hydrophobic separator as the promoting of cycles at the rate of 0.5 C, indicating that the PDA modified separator also can well restrict the dissolution of polysulfides. At rate of 1 C, both samples show a similar higher coulombic efficiency above 90%, and better cycle performance, for which is general phenomenon in Li-S batteries.⁴³ To further illustrate the reason of the superior rate performance of the cell using the hydrophilic separator, EIS tests are conducted and the results are presented in Fig. 8c and 8d. For the test cells with different separators, it can be seen that both Nyquist plots consist of one depressed semicircle at high frequencies and a straight line at low frequencies before discharge. The diameter of high frequencies semicircle refers to the charge transfer resistance, relating to the electrochemical reaction at the electrode-electrolyte, while the straight line is attributed to Warburg element, relating to the Li-ion diffusion in the electrodes.^{44,45} It is obvious that the cell using the PDA modified separator can obvious decrease the charge-transfer resistance of the sulfur cathodes as compared to bare separator, especially in the second discharge state. Therefore, it is promising from the results that the PDA modified separator with hydrophilic surface is significantly beneficial for the improvement of battery performance, especially the power capability.

Such a change in the charge-transfer resistance also can give a power explanation for the obvious dropping of capacity in the second cycle. For the cell using the bare separator, polysulfide will dissolved into the electrolyte and more and more Li₂S/Li₂S₂ will be deposited on the cathodes, leading to the loss of active materials and fast dropping of capacity. For the cell using PDA modified separator, similar dissolution of polysulfide also will happen, and there will be even more polysulfide diffused into the electrolyte due to excellent wettability of hydrophilic separator. And thus the fast decreasing of discharge capacity in the initial two cycles also can be observed. However, for the cell using PDA modified separator, the electron conductivity of electrode is well retained after discharge illustrated in the results of EIS, ensuring the fast transport of electrons from carbon to insulating Li₂S during the charge process and leading the gradual reactivation of deposited Li₂S after the initial several cycle.

Meanwhile, similar to other coating layer,⁴⁶ partial polysulfides and Li₂S can be restricted by PDA coating layer and the active materials will be gradually reutilized in the following cycles. All these factors together lead to the “V-shaped” discharge curves in the initial several cycle for the cell using the PDA modified separators.

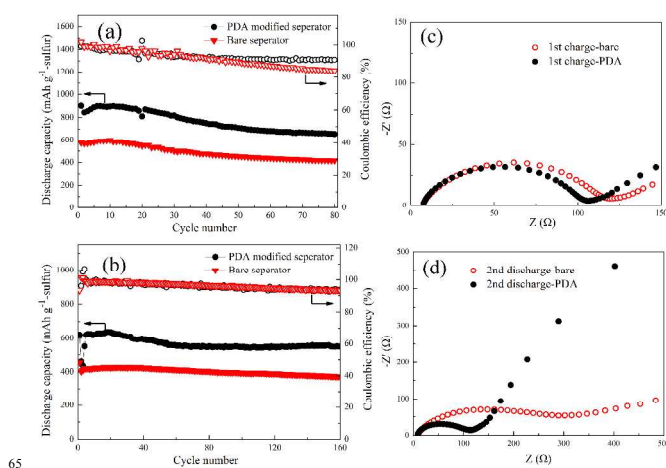


Fig. 8 The cycle performance of the cells using PDA modified separator and bare separator at the current rate of 0.5 C and 1 C (a); the Nyquist plots of the sulfur cathodes in the discharge and charge states at the rate of 0.2 C.

70 Conclusions

In conclusion, PDA modified hydrophilic separators are prepared by a simple dipping method and then successfully applied to Li-S battery. Due to the PDA modification, the surface character of the polyolefin-based separators changes from hydrophobicity to hydrophilicity, thus resulting in the improvement of uptake amounts of liquid electrolytes and ionic conductivity, accompanying with remarkably enhancement of charge/discharge capacities, cycling performance, and high-rate capability. At the 0.2 C rate, the initial discharge capacity of the cell using hydrophilic separator is 1217 mAh g⁻¹, and it can be stably retained at 1020.3 mAh g⁻¹, showing obvious advantages over the conventional hydrophobic separator. At the 1 C rate, a high reversible capacity of 548.3 mAh g⁻¹ can also be obtained, while it gets only about 373.5 mAh g⁻¹ for the cell using hydrophobic separator. More systematic studies about the effects of polydopamine amount on the surface of separators and higher sulfur loading on electrochemical properties of lithium sulfur batteries will be presented, and we expect the polydopamine modification is versatile to the improvement of electrochemical performance of lithium sulfur battery systems.

Acknowledgements

Financial Supports from NSFC (51403087, 51202094 and 51402129), the Natural Science Foundation of Jiangsu Province (BK20140563, BK20130482), the Priority Academic Program Development of Jiangsu Higher Education Institutions, and research Funds for Senior Professionals of Jiangsu University (14JDG027, 13JDG071) and Open Project of Jiangsu Key

Laboratory of Green Synthetic for Functional Materials (K201313) in China are gratefully acknowledged.

Notes and references

⁵ [†]Automotive Engineering Research Institute, Jiangsu University, Zhenjiang 212013, China

[‡]Institute of New Energy Material Chemistry, Nankai University, Tianjin 300071, China

[§]School of Chemistry and Chemical Engineering, Jiangsu Normal University, Xuzhou, Jiangsu 221116, China, E-mail: laichao@jnsu.edu.cn

This work was contributed equally by authors of G. C. Li and H. K. Jing.

- P. G. Bruce, S. A. Freunberger, L. J. Hardwick and J. M. Tarascon, *Nat. Mater.*, 2012, **11**, 19-29.
- X. P. Gao and H. X. Yang, *Energy Environ. Sci.*, 2010, **3**, 174-189.
- R. D. Rauh, K. M. Abraham, G. F. Pearson, J. K. Surprenant and S. B. Brummer, *J. Electrochem. Soc.*, 1979, **126**, 523-527.
- Z. Lin and C. D. Liang, *J. Mater. Chem. A*, 2015, **3**, 936-958.
- D. Marmorstein, T. H. Yu, K. A. Striebel, F. R. McLarnon, J. Hou and E. J. Cairns, *J. Power Sources*, 2000, **89**, 219-226.
- J. Shim, K. A. Striebel and E. J. Cairns, *J. Electrochem. Soc.*, 2002, **149**, A1321-A1325.
- Y. M. Chen, X. Y. Li, K. S. Park, J. H. Hong, J. Song, L. M. Zhou, Y. W. Mai, H. T. Huang and J. B. Goodenough, *J. Mater. Chem. A*, 2014, **2**, 10126-10130.
- X. L. Ji, K. T. Lee and L. F. Nazar, *Nat. Mater.*, 2009, **8**, 500-506.
- N. Ding, Y. W. Lum, S. F. Chen, S. W. Chien, T. S. A. Hor, Z. L. Liu and Y. Zong, *J. Mater. Chem. A*, 2015, **3**, 1853-1857.
- C. Lai, X. P. Gao, B. Zhang, T. Y. Yan and Z. Zhou, *J. Phys. Chem. C*, 2009, **113**, 4712-4716.
- H. L. Wang, Y. Yang, Y. Y. Liang, J. T. Robinson, Y. G. Li, A. Jackson, Y. Cui and H. J. Dai, *Nano Lett.*, 2011, **11**, 2644-2647.
- Y. L. Cao, X. L. Li, I. A. Aksay, J. Lemmon, Z. M. Nie, Z. G. Yang and J. Liu, *Phys. Chem. Chem. Phys.*, 2011, **13**, 7660-7665.
- G. C. Li, G. R. Li, S. H. Ye and X. P. Gao, *Adv. Energy Mater.*, 2012, **2**, 1238-1245.
- N. Jayaprakash, J. Shen, S. S. Moganty, A. Corona and L. A. Archer, *Angew. Chem. Int. Ed.*, 2011, **50**, 5904-5908.
- S. Xin, L. Gu, N. H. Zhao, Y. X. Yin, L. J. Zhou, Y. G. Guo and L. J. Wan, *J. Am. Chem. Soc.*, 2012, **134**, 18510-18513.
- L. Wang, X. M. He, J. J. Li, M. Chen, J. Gao and C. Y. Jiang, *Electrochim. Acta*, 2012, **72**, 114-119.
- Y. Z. Fu, Y. S. Su and A. Manthiram, *J. Electrochem. Soc.*, 2012, **159**, A1420-A1424.
- X. Liang, Y. Liu, Z. Y. Wen, L. Z. Huang, X. Y. Wang and H. Zhang, *J. Power Sources*, 2011, **196**, 6951-6955.
- F. Wu, J. Z. Chen, R. J. Chen, S. X. Wu, L. Li, S. Chen and T. Zhao, *J. Phys. Chem. C*, 2011, **115**, 6057-6063.
- L. F. Xiao, Y. L. Cao, J. Xiao, B. Schwenzer, M. H. Engelhard, L. V. Saraf, Z. M. Nie, G. J. Exarhos and J. Liu, *Adv. Mater.*, 2012, **24**, 1176-1181.
- D. Aurbach, E. Pollak, R. Elazari, G. Salitra, C. S. Kelley and J. Affinito, *J. Electrochem. Soc.*, 2009, **156**, A694-A702.
- X. Liang, Z. Wen, Y. Liu, M. Wu, J. Jin, H. Zhang and X. Wu, *J. Power Sources*, 2011, **196**, 9839-843.
- G. Q. Ma, Z. Y. wen, Q. S. Wang, C. Shen, J. Jin and X. W. Wu, *J. Mater. Chem. A*, 2014, **2**, 19355-19359.
- S. S. Zhang, *J. Electrochem. Soc.*, 2012, **159**, A920-A923.
- J. Shim, K. A. Striebel and E. J. Cairns, *J. Electrochem. Soc.*, 2002, **149**, A1321-A1325.
- L. X. Yuan, J. K. Feng, X. P. Ai, Y. L. Cao, S. L. Chen and H. X. Yang, *Electrochem. Commun.*, 2006, **8**, 610-614.
- D. Aurbach, E. Pollak, R. Elazari, G. Salitra, C. S. Kelley and J. Affinito, *J. Electrochem. Soc.*, 2009, **156**, A694-A702.
- B. A. Trofimov, M. V. Markova, L. V. Morozova, G. F. Prozorova, S. A. Korzhova, M. D. Cho, V. V. Annenkov, A. I. Mikhaleva, *Electrochim. Acta*, 2011, **56**, 2458-2463.
- X. Liang, Z. Y. Wen, Y. Liu, M. F. Wu, J. Jin, H. Zhang and X. W. Wu, *J. Power Sources*, 2011, **196**, 9839-9843.
- J. Sun, Y. Q. Huang, W. K. Wang, Z. B. Yu, A. B. Wang and K. G. Yuan, *Electrochim. Acta*, 2008, **53**, 7084-7088.
- J. L. Wang, Z. D. Yao, C. W. Monroe, J. Yang, and Y. N. Nuli, *Adv. Funct. Mater.*, 2013, **23**, 1194-1201.
- M. He, L. X. Yuan, W. X. Zhang, X. L. Hu and Y. H. Huang, *J. Phys. Chem. C*, 2011, **115**, 15703-15709.
- Z. W. Seh, Q. F. Zhang, W. Y. Li, G. Y. Zheng, H. B. Yao and Y. Cui, *Chem. Sci.*, 2013, **4**, 3673-3677.
- Y. M. Lee, M.-H. Ryou, M. Seo, J. W. Choi and Y. M. Lee, *Electrochim. Acta*, 2013, **113**, 433-438.
- M.-H. Ryou, Y. M. Lee, J.-K. Park and J. W. Choi, *Adv. Mater.*, 2011, **23**, 3066-3070.
- M.-H. Ryou, D. J. Lee, J. N. Lee, Y. M. Lee, J.-K. Park and J. W. Choi, *Adv. Energy Mater.*, 2012, **2**, 645-650.
- C. Y. Cao, L. Tan, W. W. Liu, J. Q. Ma and L. Li, *J. Power Sources*, 2014, **248**, 224-229.
- H. Lee, S. M. Dellatore, W. M. Miller and P. B. Messersmith, *Science*, 2007, **318**, 426-430.
- Y. L. Liu, K. L. Ai and L. H. Lu, *Chem. Rev.*, 2014, **114**, 5057-5115.
- Q. Ye, F. Zhou and W. Liu, *Chem. Soc. Rev.*, 2011, **40**, 4244-4258.
- J. J. Wilker, *Nat. Chem. Biol.*, 2011, **7**, 579-580.
- F. Bernsmann, V. Ball, F. Addiego, A. Ponche, M. Michel, J. J. Almeida Gracio, V. Toniazio and D. Ruch, *Langmuir*, 2011, **27**, 2819-2825.
- J. Bruckner, S. Thieme, H.T. Grossmanr, S. Dorfler, H. Althues and S. Kaskel, *J. Power Sources*, 2014, **268**, 82-87.
- X. Gu, Y. Wang, C. Lai, J. Qiu, S. Li, Y. Hou, W. Martens, N. Mahmood and S. Zhang, *Nano Res.*, 2015, **8**, 129-139.
- W. G. Wang, X. Wang, L. Y. Tian, Y. L. Wang and S. H. Ye, *J. Mater. Chem. A*, 2014, **2**, 4316-4323.
- H. B. Yao, K. Yan, W. Y. Li, G. Y. Zheng, D. S. Kong, Z. W. She, V. K. Narasimhan, Z. Liang and Y. Cui, *Energy Environ. Sci.*, 2014, **7**, 3381-3390.